PROCEEDINGS OF SPIE

SPIEDigitalLibrary.org/conference-proceedings-of-spie

A monolithic integrated low-threshold Raman silicon laser

Rong, Haisheng, Xu, Shengbo, Cohen, Oded, Raday, Omri, Lee, Mindy, et al.

Haisheng Rong, Shengbo Xu, Oded Cohen, Omri Raday, Mindy Lee, Vanessa Sih, Mario Paniccia, "A monolithic integrated low-threshold Raman silicon laser," Proc. SPIE 6898, Silicon Photonics III, 68980J (25 February 2008); doi: 10.1117/12.766811

SPIE.

Event: Integrated Optoelectronic Devices 2008, 2008, San Jose, California, United States

Downloaded From: https://www.spiedigitallibrary.org/conference-proceedings-of-spie on 02 Dec 2021 Terms of Use: https://www.spiedigitallibrary.org/terms-of-use

A monolithic integrated low-threshold Raman silicon laser

Haisheng Rong[a], Shengbo Xu[a], Oded Cohen[b], Omri Raday[b], Mindy Lee[a], Vanessa Sih[a], and Mario Paniccia[a]

[a]Intel Corporation, 2200 Mission College Blvd, SC12-326, Santa Clara, CA 95054, USA
[b]Intel Corporation, S. B. I. Park Har Hotzvim, Jerusalem, 91031, Israel

ABSTRACT

We present a monolithic integrated low-threshold Raman silicon laser based on silicon-on-insulator (SOI) rib waveguide ring cavity with an integrated p-i-n diode. The laser cavity consists of a race-track shaped ring resonator connected to a straight bus waveguide via a directional coupler which couples both pump and signal light into and out of the cavity. Reverse biasing the diode with 25V reduces the free carrier lifetime to below 1 ns, and stable, single-mode, continuous-wave (CW) Raman lasing is achieved with threshold of 20mW, slope efficiency of 28%, and output power of 50mW. With zero bias voltage, a lasing threshold of 26mW and laser output power >10mW can be obtained. The laser emission has high spectral purity with a side-mode suppression of >80dB and laser linewidth of <100 kHz. The laser wavelength can be tuned continuously over 25 GHz. To demonstrate the performance capability of the laser for gas sensing application, we perform absorption spectroscopy on methane at 1687 nm using the CW output of the silicon Raman laser. The measured rotationally-resolved direct absorption IR spectrum agrees well with theoretical prediction. This ring laser architecture allows for on-chip integration with other silicon photonics components to provide an integrated and scaleable monolithic device. By proper design of the ring cavity and the directional coupler, it is possible to achieve higher order cascaded Raman lasing in silicon for extending laser wavelengths from near IR to mid IR regions.

Keywords: silicon photonics, silicon laser, optoelectronics integration, two photon absorption, free-carrier absorption, stimulated Raman scattering, Raman laser, laser spectroscopy, gas sensing.

1. INTRODUCTION

Silicon photonics offers promising low-cost optoelectronic solutions for a wide range of applications from telecommunications and interconnects to optical sensing and biomedical applications[1-6]. In recent years, rapid progress has been made in developing various silicon-based photonics building blocks for these applications. In particular, nonlinear optical effect such as stimulated Raman scattering (SRS) has been demonstrated as a successful approach for achieving both amplification and lasing in silicon[7-20]. Due to the high nonlinearity and strong light confinement in silicon waveguides, efficient and compact nonlinear optical devices can be realized on silicon chips. The key challenge is to fabricate silicon waveguides with very low optical losses. The nonlinear loss due to two photon absorption (TPA) induced free carrier absorption (FCA) is the major contributor when high power density is present in the waveguides to create nonlinear effects[21-22]. By integrating a p-i-n diode into the silicon waveguide, the FCA can be significantly reduced when reverse biasing the diode and efficient Raman amplification and lasing can be achieved on a silicon chip. Raman lasers have the ability to generate coherent light in wavelength regions which are not easily accessible with other conventional types of lasers. However, due to the inefficient nonlinear SRS process, high pump powers are typically required to reach lasing threshold. Most the Raman lasers, therefore, operate in pulsed mode. CW Raman lasing has been achieved either using high-Q resonant cavities making use of the resonant enhancement effect[23,24], or in optical fibres[25] where the light is tightly confined and the interaction length can be over of several kilometres. Silicon Raman lasers take advantages of the high Raman gain in silicon and strong light confinement due to its high refractive index. In addition, due to its compact cavity size, also the resonance enhancement of the pump power can be utilized. Combining all these benefits and proper cavity design, we show here that low-threshold silicon Raman laser can be achieved in CW operation. From the output power we estimate that the intra cavity power at the Stokes wavelength can be strong enough to generate higher order cascaded

Silicon Photonics III, edited by Joel A. Kubby, Graham T. Reed
Proc. of SPIE Vol. 6898, 68980J, (2008) · 0277-786X/08/$18 · doi: 10.1117/12.766811

Downloaded From: https://www.spiedigitallibrary.org/conference-proceedings-of-spie on 02 Dec 2021
Terms of Use: https://www.spiedigitallibrary.org/terms-of-use

lasing. This would enable extending the lasing wavelength into the mid-IR region where low-cost, compact, and room temperature lasers are in high demand for many applications ranging from high-resolution and ultra-sensitive detection of molecules for trace-gas sensing, environmental monitoring, and biomedical analysis, to industrial process control and free-space communications[26].

2. DEVICE DESIGN AND FABRICATION

The ring laser resonator is constructed from a low-loss silicon-on-insulator (SOI) rib waveguide in a race-track shape (Fig. 1). A bus waveguide is connected with the ring cavity via a directional coupler which couples both pump and signal laser light into and out of the cavity. The coupling ratio can be varied by changing the gap and/or length of the coupler[27] to achieve desired coupling for the pump and lasing wavelengths. To make efficient use of the pump and achieve low lasing threshold, the coupler was designed so that it is close to critical coupling for the pump wavelength and has a low coupling for the lasing wavelength. The coupling ratio and optical propagation loss of the waveguide can be determined experimentally by analyzing the transmission spectrum of the ring resonators[28].

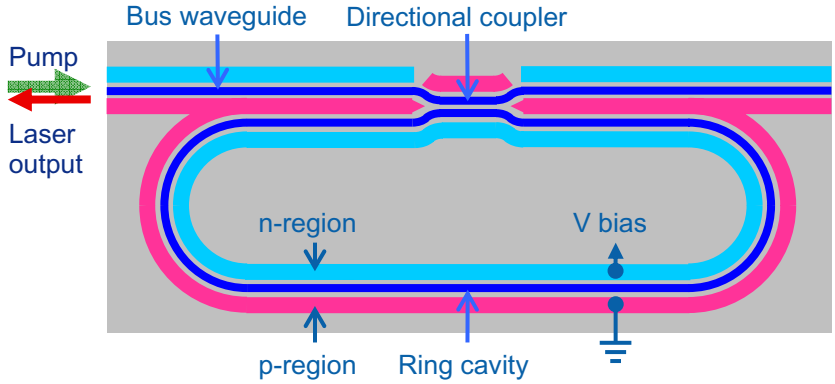

Figure 1: Layout of the silicon Raman ring laser cavity with a p-i-n diode structure along the waveguides.

The silicon rib waveguide is fabricated on the (100) surface of a SOI substrate using standard photolithographic patterning and reactive ion etching techniques. A cross-section schematic for the directional coupler region of a typical p-i-n ring cavity is shown in Fig. 2. The designed rib waveguide dimensions are: rib width (W) 1.5 μm, height (H) 1.55 μm, and etch depth (h) 0.75 μm. The gap (d) between the two waveguides in the coupler is around 0.7 μm and the coupling length varies between 700 and 1100 um to obtain different coupling ratios for both pump and signal wavelengths. The total length of the ring cavity is 3 cm and the bend radius is 400 μm (Fig. 1). The straight sections of the waveguide are oriented along the [011] crystallographic direction.

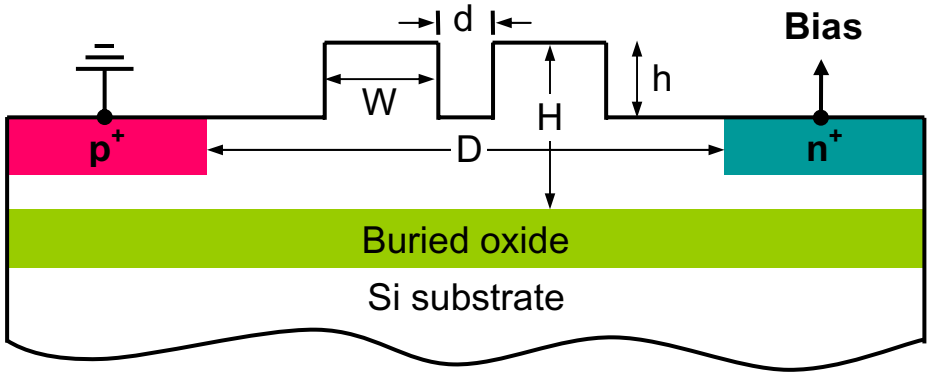

Figure 2: A cross-section schematic of the coupler region in the ring resonator.

Downloaded From: https://www.spiedigitallibrary.org/conference-proceedings-of-spie on 02 Dec 2021
Terms of Use: https://www.spiedigitallibrary.org/terms-of-use

A p-i-n diode structure is designed to reduce the nonlinear optical loss due to TPA induced FCA. The p-i-n structure is formed by implanting boron and phosphorus in the slab on either side of the rib waveguide with a doping concentration of 1×10^{20} cm^{-3} to form p and n regions as highlighted in Fig. 1. To reduce the coupling loss and achieve consistent coupling, the coupler gap is filled with boron phosphorous silicon glass (BPSG) film thermally reflowed to eliminate voids in this region. The p and n doped regions are designed to be 2.3 μm away from the rib waveguide to avoid additional losses due to the heavy doping concentration.

3. DEVICE CHARACTERIZATION

The ring laser resonators are first characterized by measuring the optical propagation loss and the coupling ratios at both pump and signal wavelengths and for both TE and TM polarizations. The average optical loss of the race track ring is determined to be 0.2 dB/cm by measuring its transmission spectrum using a tunable laser. The p-i-n diode has negligible contribution to the linear propagation loss. The total loss in the coupler region is measured to be less than 0.1 dB for all the various devices, and the bend regions of the race track are found to have negligible contribution to the total round trip loss of the ring cavity.

To characterize the performance of the p-i-n diode in reducing the free carrier lifetime, the free carrier lifetimes as a function of applied reverse bias voltages are examined. We measure the optical power transmission through a 4.6 cm long waveguide fabricated on the same test chip as the ring cavities as a function of the coupled input power. By fitting the nonlinear transmission curves we can determine the carrier lifetime using the method described in ref. 11 with the following parameters: linear loss 0.2 dB/cm, TPA coefficient 0.5 cm/GW, and FCA cross section 1.45×10^{-17} cm^2. The intrinsic (open circuit) effective carrier lifetime is measured to be ~15.3 ns. With the p and n terminals shorted together (or zero bias), the internal field between the p and n regions is sufficient to reduce the carrier lifetime to ~4.7 ns. With a reverse bias of 25V the carrier lifetime goes down to ~ 0.32ns. This is instrumental for enabling low threshold and high output laser devices. These results have been verified by using an independent pump-probe measurement technique as described in ref. 22.

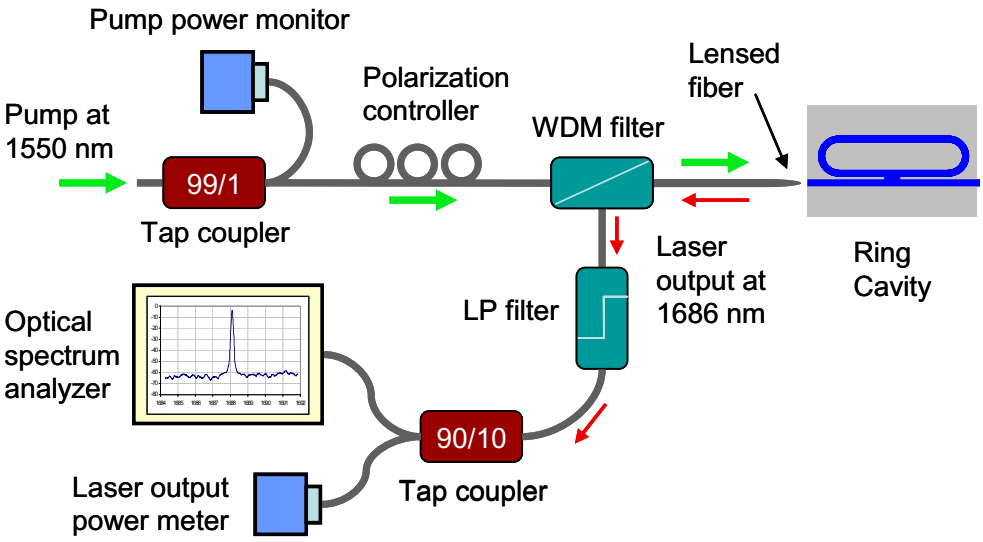

Figure 3: Schematic setup of the silicon ring laser experiment.

Figure 3 is a schematic of the ring laser experimental setup. A CW external cavity diode laser at 1550 nm amplified by an erbium-doped fiber amplifier is used as the pump. The pump beam passes through a polarization controller followed by a thin-film-based WDM filter and is coupled into the waveguide cavity by a lensed fiber. The Raman laser output at 1686 nm is coupled back into the same lensed fiber, and separated from the pump by the WDM filter

Downloaded From: https://www.spiedigitallibrary.org/conference-proceedings-of-spie on 02 Dec 2021
Terms of Use: https://www.spiedigitallibrary.org/terms-of-use

followed by an additional long wavelength pass (LP) filter before being detected by a power meter or optical spectrum analyzer. The coupling loss between the lensed fiber and the waveguide is measured to be 4 dB and the total insertion loss of the WDM filter and the long-pass filter is 1 dB.

Figure 4 plots the Raman silicon ring laser output power as a function of the input pump power coupled into the bus waveguide for a 3 cm long ring cavity with different bias voltages applied to the p-i-n diode at room temperature. In the experiment, the pump beam polarization is adjusted with a polarization controller and its wavelength is fine tuned to the cavity resonance to take advantage of the cavity enhancement and maximize the laser output. The silicon Raman laser frequency is 15.6 THz red-shifted from the pump laser. The evanescent coupler's coupling ratios for the pump and Stokes wavelength are 30% and 12%, respectively. Note that a total linear loss of 0.6 dB for a 3 cm cavity would require a coupling ratio of 13% for critical coupling and maximum cavity enhancement effect. However, the cavity loss slightly increases with the pump power due to the residual FCA effect. We chose an over coupling for the pump to offset this loss increase. A coupling ratio of 30% here corresponds to a cavity enhancement factor of about 6, i.e., the intra cavity pump power is about 6 times of the coupled input power. With a 25V reverse bias, which sweeps out the free carriers most efficiently, the lasing threshold is measured to be ~20 mW with a maximum output power of ~50 mW. The slope efficiency for this configuration around the lasing threshold is calculated to be ~28%. As the bias voltage is lowered, the laser output begins to saturate earlier due to the relatively longer effective carrier lifetime. However, the lasing threshold changes only slightly because the TPA is much weaker at the lower pump powers around threshold.

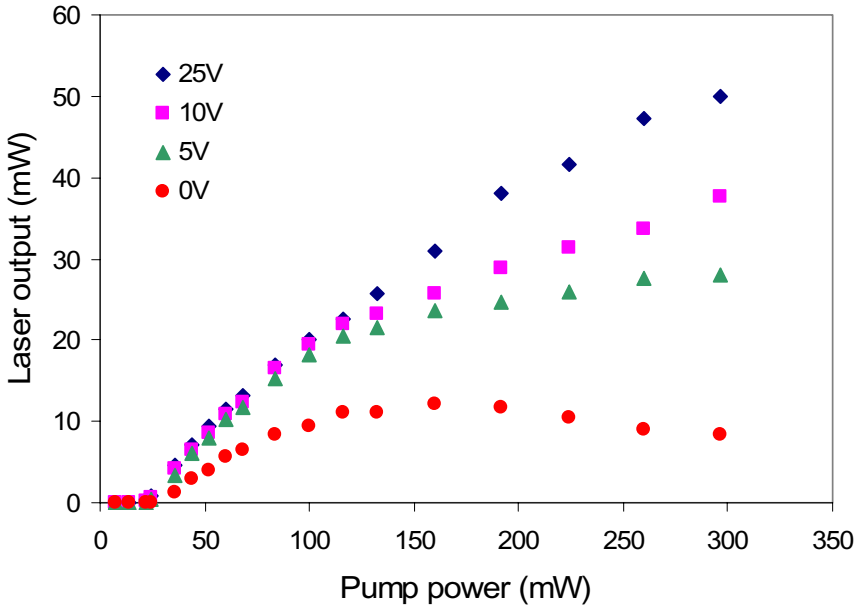

Figure 4: Silicon Raman laser output power as a function of the input pump power for a 3 cm long ring cavity with different bias voltages applied to the p-i-n diode at room temperature.

As a result of the reduced effective carrier lifetime and linear optical loss in the ring cavity, Fig. 4 also shows that even when no voltage is applied, the silicon Raman laser can still be operated in CW mode with a relatively low threshold of 26 mW and a respectable saturation output power exceeding 10 mW. In this situation, the laser does not need any external electrical power supply, enabling a stand-alone all optical device which is particularly attractive where no electrical power supply is accessible or allowed, such as in remote sensing applications.

The laser output spectrum is measured using a grating based optical spectrum analyzer with 0.01 nm resolution. As shown in Fig. 5, the laser is single mode with a side mode suppression ratio of >80 dB. For this measurement, the pump laser is at 1430.5 nm to obtain lasing at 1545.5 nm where the optical spectrum analyzer has lower noise floor. The laser spectral linewidth is measured more accurately using a delayed heterodyne technique[29] and a typical value of <100 kHz is obtained.

Downloaded From: https://www.spiedigitallibrary.org/conference-proceedings-of-spie on 02 Dec 2021
Terms of Use: https://www.spiedigitallibrary.org/terms-of-use

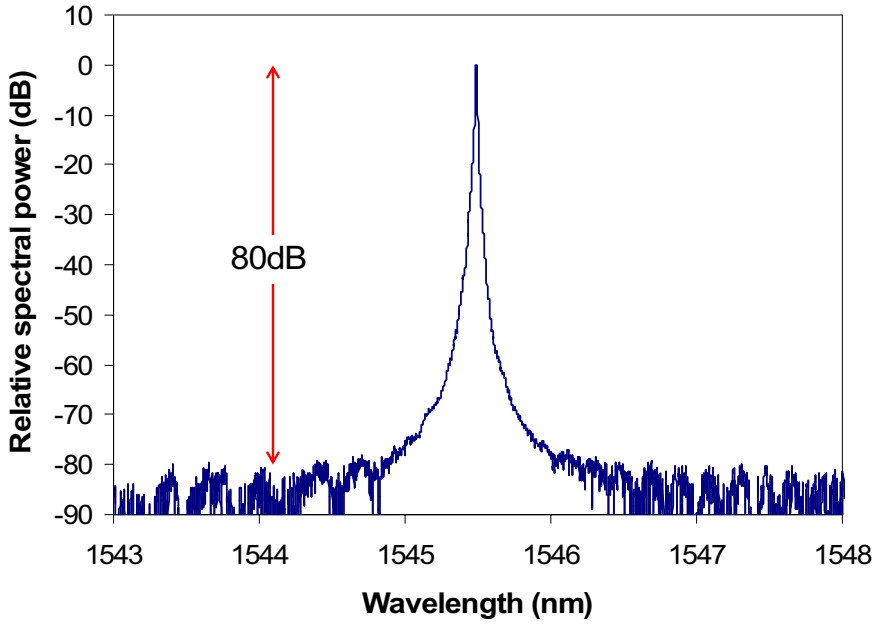

Figure 5: Silicon Raman laser spectrum measured with a grating based optical spectrum analyser with a resolution of 0.01nm, showing a side mode suppression ratio of > 80 dB. The pump is at 1430.5 nm and lasing wavelength is 1545.5 nm.

4. SPECTROSCOPY EXPERIMENT

Trace and/or remote gas sensing is an important application of near and mid IR lasers enabled by the fact that IR-active rotational-vibrational transitions of many molecules provide unique "fingerprint" absorption patterns in these regions[30]. To demonstrate the performance and capability of the silicon Raman laser for this type of application, we performed direct absorption spectroscopy experiments on methane, one of the major greenhouse gases, having characteristic absorption patterns in the wavelength region covered by the silicon Raman laser.

The setup for the absorption spectroscopy experiment is shown in Fig. 6. The Raman laser output is split into three beams. One reference beam is sent into a photo detector directly, while the other two beams are sent through a methane gas cell and a silicon waveguide etalon, before reaching the photo detectors. The methane cell used in this experiment is 30 cm long and has a gas pressure of 10 Torr. The silicon waveguide is 8 cm long with polished facets forming a Fabry-Perot (FP) etalon. The periodic FP pattern from the silicon etalon serves as frequency marks to calibrate the wavelength scan. A pump wavelength of 1548 nm is used to generate Stokes lasing wavelength at 1684 nm to probe a distinctive group of methane absorption lines near this wavelength. By slowly scanning the pump laser, we can obtain continuous tuning of the Raman laser wavelength over the absorption line profile.

Figure 7 plots the methane cell transmission, normalized to the reference photo detector, as a function of the laser wavelength. The transmission of the silicon etalon is recorded simultaneously and is shown in the lower part of Fig. 7. From the continuous FP pattern and the FSR of the silicon waveguide etalon of 540 MHz, we estimate that a mode-hop free tuning range of 25 GHz can be obtained, which is sufficient to cover the width of typical molecular IR absorption profiles at room temperature. Wider mode-hop free tuning could be obtained by controlling the temperature of the laser chip in sync with the scan of the pump laser wavelength. The solid line in Fig. 6 is the calculated IR absorption line profile for methane using the HITRAN 2004 database[31]. The measured absorption profile agrees well with the theoretically predicted one.

Downloaded From: https://www.spiedigitallibrary.org/conference-proceedings-of-spie on 02 Dec 2021
Terms of Use: https://www.spiedigitallibrary.org/terms-of-use

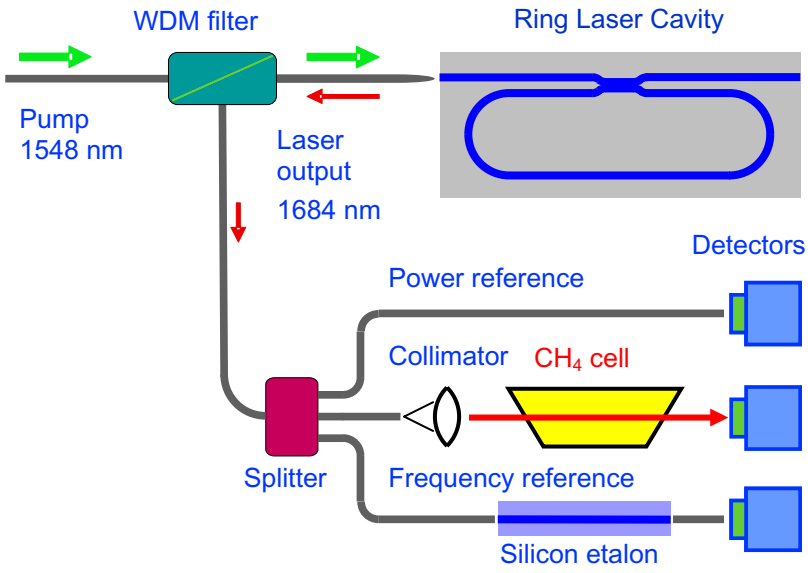

Figure 6: Schematic setup for methane absorption spectroscopy using silicon Raman laser.

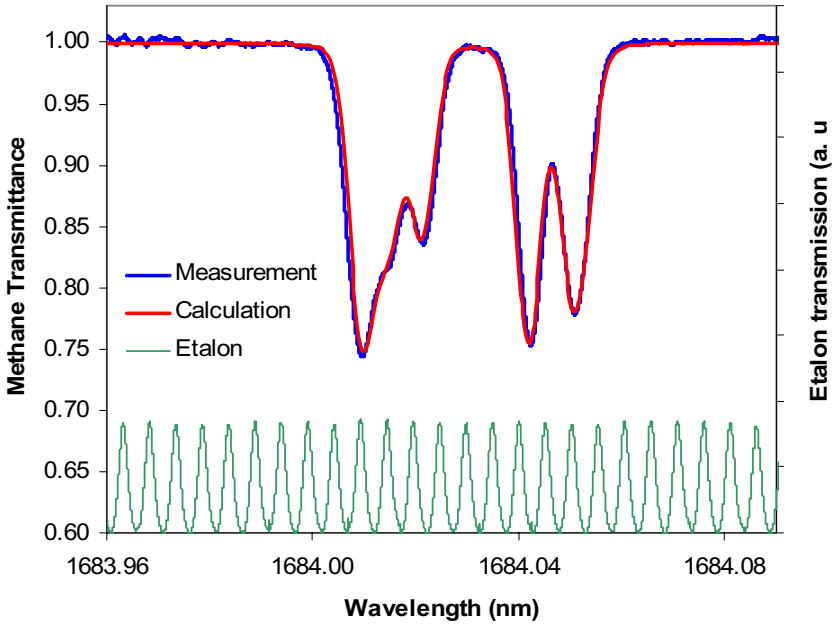

Figure 7: Methane absorption spectrum (blue) at 1684 nm measured with the silicon Raman laser. The solid curve (red) is a calculation based on HITRAN database. The transmission spectrum (green) of a silicon etalon with a FSR of 540 MHz is taken simultaneously and provides frequency calibration marks.

Downloaded From: https://www.spiedigitallibrary.org/conference-proceedings-of-spie on 02 Dec 2021
Terms of Use: https://www.spiedigitallibrary.org/terms-of-use

5. SUMMARY

In this paper we have presented a chip-scale Raman silicon laser based on SOI rib waveguide with an integrated p-i-n diode in a ring cavity configuration. We achieved single-mode CW lasing with a low-threshold of 20 mW. The laser output power exceeds 50mW at 25V bias voltage, and the slope efficiency is 28% near the threshold. With zero bias voltage, we obtained lasing threshold of 26mW and laser output power >10mW. The laser output has high spectral purity with a side-mode suppression of greater than 80 dB and a linewidth of less than 100 kHz. This ring cavity design allows dimension scalability and on-chip integration with other silicon based optical components. The realization of low-threshold monolithic integrated Raman silicon lasers represents a significant step towards producing practical and low-cost silicon based photonic devices. Taking advantage of the extra-ordinary spectral purity of the silicon Raman laser, we performed direct absorption spectroscopy experiment on methane to demonstrate the performance and capability of the laser in gas sensing application. The unique features of the silicon Raman laser, combined with its low-cost fabrication, could enable entirely new applications for silicon photonics in areas such as coherent optical communications, spectroscopy, and optical sensing. Similar to fibre Raman ring or micro-cavity lasers[32, 33], cascaded lasing is also possible in silicon Raman lasers[34]. This would allow extending of the lasing wavelength into the mid infrared region where a suitable room temperature semiconductor laser is in high demand for many applications ranging from high-resolution and ultra-sensitive detection of molecules for trace gas analysis, pollution and toxic gas monitoring, and biomedical sensing, to free-space optical communications.

ACKNOWLEDGEMENTS

The authors would like to acknowledge Y.-H. Kuo for contributions in ring resonator development; A. Alduino, D. Tran, J. C. Jimenez, N. Izhaky, N. Ziharev and J. Ngo for assistance in device fabrication and sample preparation. R. Jones, A. Liu, G. T. Reed for technical discussions.

REFERENCES

1. G. T. Reed, "The optical age of silicon," *Nature* **427**, 615−618 (2004).
2. L. Pavesi and D. J. Lockwood, *Silicon Photonics* (Springer-Verlag, Heidelberg, 2004).
3. G. T. Reed and A. P. Knights, *Silicon Photonics: An Introduction* (John Wiley, Chichester, UK, 2004).
4. L. Pavesi and G. Guillot, *Optical Interconnects - the silicon approach* (Springer-Verlag, Heidelberg, 2006).
5. E. Chow, A. Grot, L. W. Mirkarimi, M. Sigalas, and G. Girolami, "Ultracompact biochemical sensor built with two-dimensional photonic crystal microcavity," *Opt. Lett.* **29**, 1093-1095 (2004).
6. B. Schmidt, V. Almeida, C. Manolatou, S. Preble, and M. Lipson, "Nanocavity in a silicon waveguide for ultrasensitive nanoparticle detection," *Appl. Phys. Lett.* **85**, 4854-4856 (2004).
7. A. Liu, H. Rong, M. Paniccia, O. Cohen, and D. Hak, "Net optical gain in a low loss silicon-on-insulator waveguide by stimulated Raman scattering," *Opt. Express* **12**, 4261-4267 (2004).
8. Q. Xu, V. Almeida, M. Lipson, "Time-resolved study of Raman gain in highly confined silicon-on-insulator waveguides," *Opt. Express* **12**, 4437-4442 (2004).
9. T. K. Liang and H. K. Tsang, "Efficient Raman amplification in silicon-on-insulator waveguides," *Appl. Phys. Lett.* **85**, 3343-3345 (2004).
10. O. Boyraz and B. Jalali, "Demonstration of 11 dB fiber-to-fiber gain in a silicon Raman amplifier," *IEICE Elect. Express* **1**, 429-434 (2004).
11. R. Jones, H. Rong, A. Liu, A. W. Fang, M. Paniccia, D. Hak, and O. Cohen, "Net continuous-wave optical gain in a low loss silicon-on-insulator waveguide by stimulated Raman scattering," *Opt. Express* **13**, 519-525 (2005).
12. X. Chen, N. C. Panoiu, and R. M. Js. Osgood, "Theory of Raman-Mediated Pulsed Amplification in Silicon-Wire Waveguides," *IEEE J. Quant. Electron.* **42**, 160-170 (2006).

Downloaded From: https://www.spiedigitallibrary.org/conference-proceedings-of-spie on 02 Dec 2021
Terms of Use: https://www.spiedigitallibrary.org/terms-of-use

13. Y. Liu and H. K. Tsang, "Nonlinear Absorption and Raman Gain in Helium Ion Implanted Silicon," *Opt. Lett.* **31**, 1714-1716 (2006).
14. Sasan Fathpour, Ozdal Boyraz, Dimitri Dimitropoulos, and Bahram Jalali, "Demonstration of CW Raman Gain with Zero Electrical Power Dissipation in p-i-n Silicon Waveguides," *Conference on Lasers and Electro-Optics*, Paper CMK3, Long Beach, CA, May 2006.
15. O. Boyraz and B. Jalali, "Demonstration of a silicon Raman laser," *Opt. Express* **12**, 5269-5273 (2004).
16. H. Rong, A. Liu, R. Jones, O. Cohen, D. Hak, R. Nicolaescu, A. Fang, and M. Paniccia, "An all-silicon Raman laser," *Nature* **433**, 292-294 (2005).
17. H. Rong, R. Jones, A. Liu, O. Cohen, D. Hak, A. Fang, and M. Paniccia, "A continuous-wave Raman silicon laser," *Nature* **433**, 725-728 (2005).
18. A. Liu, H. Rong, R. Jones, O. Cohen, D. Hak, and M. Paniccia, "Optical Amplification and Lasing by Stimulated Raman Scattering in Silicon Waveguides," *J. Lightwave Tech.* **24**, 1440-1455 (2006).
19. H. Rong, R. Jones, A. Liu, O. Cohen, D. Hak, and M. Paniccia. "Characterization of a silicon Raman laser," *Proc of SPIE* **5931**, 59310R 1-9 (2006).
20. H. Rong, Y.-H. Kuo, S. Xu, A. Liu, R. Jones, M. Paniccia, O. Cohen, and O. Raday, "Monolithic integrated Raman silicon laser," Opt. Express 14, 6705-6712 (2006).
21. T. K. Liang and H. K. Tsang, "Role of free carriers from two-photon absorption in Raman amplification in silicon-on-insulator waveguides," *Appl. Phys. Lett.* **84**, 2745-2747 (2004).
22. H. Rong, A. Liu, R. Nicolaescu, M. Paniccia, O. Cohen, and D. Hak, "Raman gain and nonlinear optical absorption measurement in a low loss silicon waveguide," *Appl. Phys. Lett.* **85,** 2196-2198 (2004).
23. J. K. Brasseur, K. S. Repasky, and J. L. Carlsten, "Continuous-wave Raman laser in H_2," *Opt. Lett.* **23**, 367-369 (1998).
24. S. M. Spillane, T. J. Kippenberg, and K. J. Vahala, "Ultralow-threshold Raman laser using a spherical dielectric microcavity," *Nature* **415**, 621-623 (2002).
25. E.M. Dianov, and A.M. Prokhorov, "Medium-power CW Raman fiber lasers," *IEEE J. Sel. Topics Quantum Electron.* **6**, 1022-1028 (2000).
26. I. T. Sorokina and K. L. Vodopyanov, (eds.) *Solid-state mid-infrared laser sources* (Springer-Verlag, Berlin/Heidelberg, 2003).
27. W.R. Headley, G.T. Reed, S. Howe, A. Liu, and M. Paniccia, "Polarization-independent optical racetrack resonators using rib waveguides on silicon-on-insulator," *Appl. Phys. Lett.* **85**, 5523-5525 (2004).
28. R. Adar, Y. Shani, C. H. Henry, R. C. Kistler, G. E. Blonder, and N. A.Olsson, "Measurement of very low-loss silica on silicon waveguide with a ring resonator," *Appl. Phys. Lett.* **58**,. 444-445 (1991).
29. D. M. Baney and W. V. Sorin, *Fiber Optic Test and Measurement*, D. Derickson, ed. (Prentice-Hall, Upper Saddle River, NJ, 1998), pp. 169–219.
30. F. K. Tittel, D. Richter, and A. Fried, "Mid-Infrared Laser Applications in Spectroscopy," in *Solid-State Mid-Infrared Laser Sources*, I. T. Sorokina, and K. L. Vodopyanov, eds. (Springer-Verlag, Berlin/Heidelberg, 2003), pp. 445-510.
31. L. S. Rothman, et al., "The HITRAN 2004 molecular spectroscopic database," *Journal of Quantitative Spectroscopy & Radiative Transfer* **96**, 139-204 (2005).
32. J. G. Naeini, and K. Ahmad, "Raman fiber laser with two parallel couplers," *Opt. Eng.* **44**, 064203 (2005).
33. T. J. Kippenberg, S. M. Spillane, B. Min, and K. J. Vahala, "Theoretical and Experimental Study of Stimulated and Cascaded Raman Scattering in Ultrahigh-Q Optical Microcavities," *IEEE J. Sel. Top. Quant. Electron.* **10**, 1219-1228 (2004).
34. M. Krause, R. Draheim, H. Renner, and E. Brinkmeyer, "Cascaded silicon Raman lasers as mid-infrared sources," *Elec. Lett.* **42** 1224-1226 (2006).

Downloaded From: https://www.spiedigitallibrary.org/conference-proceedings-of-spie on 02 Dec 2021
Terms of Use: https://www.spiedigitallibrary.org/terms-of-use